Journal of Geodesy (1997) 71: 486–501

Journal of Geodesy

A canonical theory for short GPS baselines.
Part III: the geometry of the ambiguity search space

P. J. G. Teunissen

Delft Geodetic Computing Centre (LGR), Faculty of Geodesy, Delft University of Technology, Thijsseweg 11, 2629 JA Delft, The Netherlands

Received: 16 July 1996 / Accepted: 14 November 1996

Abstract. This contribution is the third of four parts. Based on the gain-number concept, canonical forms will be presented of the ambiguity search spaces of the geometry-based model, the time-averaged model, and the geometry-free model. These forms reveal the intrinsic geometry of the search spaces and allow one to study their size, shape, and orientation as function of data precision, sampling rate, satellite redundancy, and change in receiver-satellite geometry. The canonical forms are also used to address the problem of search halting. The phenomenon of search halting is explained and it is shown how decorrelating ambiguity transformations can largely eliminate this computational burden.

1 Introduction

In this contribution we will analyze the geometry of the ambiguity search space. The present study is a continuation of Teunissen (1996a, 1996b), which will henceforth be referred to as *Part I* and *Part II*, respectively. Although our analysis is restricted to the single-baseline model, we consider three different versions of it. They are the geometry-based model, the time-averaged model, and the geometry-free model. For the *geometry-based* model, the linearized set of double-differenced (DD) observation equations reads as

$$\begin{aligned} D^T\phi_j(i) &= D^TA_ib + \lambda_j a_j \ , \\ D^Tp_j(i) &= D^TA_ib \ , \end{aligned} \qquad (1)$$

with $j = 1, 2$ and where $i = 1, \ldots, k$ denotes the epoch number and k equals the total number of epochs; ϕ_1, ϕ_2, p_1 and p_2 are the m-vectors containing the (observed minus computed) metric *single-differenced* (SD) phase and code observables on L_1 and L_2; D^T is the $(m-1)\times m$ DD matrix operator; A_i is the $m \times 3$ SD design matrix that captures the relative receiver-satellite geometry at epoch i; b is the 3-vector that contains the unknown increments of the three-dimensional baseline; λ_1 and λ_2 are the wavelengths of L_1 and L_2; and a_1 and a_2 are the two $(m-1)$-vectors that contain the unknown *integer* DD ambiguities. Time correlation is assumed to be absent and the time-invariant weight matrix (inverse variance matrix) at epoch i is assumed to be given as the block diagonal matrix

$$Q^{-1} = \mathrm{diag}(\alpha_1, \alpha_2, \beta_1, \beta_2) \otimes \left(D^TD\right)^{-1}, \qquad (2)$$

where '$\otimes$' denotes the Kronecker product. The scalars α_1, α_2, β_1, and β_2 are the weights of the L_1 and L_2 phase and code observables.

The *time-averaged* model follows from taking the time average of the vectorial observation equations of Eq. (1). The *geometry-free* model follows from the geometry-based model if we disregard the presence of the receiver-satellite geometry. Hence it follows if we replace A_ib in Eq. (1) by the SD range vector r_i.

Motivated by the purpose of ambiguity fixing, the gain-number concept was introduced in *Part I*. The gain numbers were defined as the stationary values of the variance ratio of baseline precision before and after ambiguity fixing. Thus the gain numbers measure the improvement in baseline precision due to the fixing of the ambiguities. With the gain number concept, we were able to give a complete canonical description of the baseline precision. In *Part II* we studied the precision and correlation of the ambiguities. We also analyzed the celebrated widelane ambiguity and showed that its precision is not per se better than the precision of the L_1 and L_2 ambiguities. Fortunately, the conditions for which they have a better precision are usually satisfied in practice. It was also shown, through the gain numbers, how the ambiguity precision and correlation is affected by the receiver-satellite geometry. One of the results obtained was that the ambiguities are highly correlated when the gain numbers are large and that one cannot expect the correlation to decrease significantly over time if only short observation time-spans are used.

In the present contribution, we will give a canonical description of the size, shape, and orientation of the ambiguity search space. This is done for all three of the mentioned single-baseline models. In Sect. 2 we intro-

duce the ambiguity search space and confront the reference-satellite dependency of the DD ambiguities. In Sect. 3 we present a way of describing the DD grid such that it becomes independent of the arbitrary choice of reference satellite. It allows us to concentrate on the truly intrinsic properties of the search space.

In Sects. 4 and 5 the canonical forms are given of the various search spaces. The single-frequency case is considered in Sect. 4 and the dual-frequency case in Sect. 5. The canonical forms show for each of the individual cases how the size, shape, and orientation depend on the observation weights, on the number of satellites tracked, on the number of observation epochs used, and on the change over time of the receiver-satellite geometry.

In Sect. 6 we consider the problem of search halting which is typically experienced when computing the DD integer least-squares ambiguities. The nature of the search halting is explained by means of the results of the previous two sections. We also study the use of the widelane ambiguity and show how it affects the shape of the search space. Finally we show why decorrelating ambiguity transformations in general help to diminish the problem of search halting.

2 The ambiguity search space

The process of GPS ambiguity resolution can be divided into two distinct parts:

1. the ambiguity *estimation* problem,
2. the ambiguity *validation* problem.

The estimation part addresses the problem of finding optimal estimates for the ambiguities. Since the principle of least squares is employed, the task is to find the least-squares solution for the unknown integer ambiguities. The second part is concerned with the validation of the estimated integer ambiguities. The validation part is of importance in its own right and quite distinct from the estimation part. Namely, one will always be able to compute an integer least-squares solution, whether it is of poor quality or not. The question addressed by the validation part is therefore, whether the quality of the computed integer least squares solution is such that one is also willing to accept this solution.

In both the estimation and the validation of the integer ambiguities, a central role is played by the quadratic form

$$T(a) = (\hat{a} - a)^T Q_{\hat{a}}^{-1} (\hat{a} - a)\,, \tag{3}$$

in which $\hat{a}$ denotes the real-valued least squares estimate of the ambiguity vector and $Q_{\hat{a}}$ denotes its variance matrix. In case of validation, one infers whether the most likely integer ambiguities are sufficiently likely and whether the less likely integer values differ sufficiently in likelihood from the most likely values. With the principle of least squares, assuming normally distributed data, the most likely integer ambiguities are given by the integer least-squares solution, denoted by $\check{a}$. The inference of the likelihood of the integer least-squares solution is therefore based on $T(\check{a})$. In a similar way, the quadratic form Eq. (3) is used to infer the likelihood of the less likely integer solutions, for instance the second most likely solution. Since $T(\check{a})$ compares the *real-valued* least-squares ambiguities with the *integer* least-squares ambiguities, it implicitly compares to what extent the data is consistent with the model when either the integer constraints $a \in Z^{2(m-1)}$ are included in the model or when they are excluded. When the integer constraints are included, the parameter estimates are usually referred to as the 'fixed' solution. Without these constraints, they are usually referred to as the 'float' solution. That $T(\check{a})$ indeed measures to what degree the data is consistent with the model when the integer constraints are included or when not, follows from the fact that it equals the difference of two weighted sum of squares, one in the 'fixed' least-squares residuals and the other in the 'floated' least-squares residuals. For our single GPS baseline model, they read as

$$\begin{cases} T(\hat{e}) &= \sum_{i=1}^{k} \sum_{j=1}^{2} \alpha_j \parallel \hat{e}_{\phi_j}(i) \parallel^2 + \beta_j \parallel \hat{e}_{p_j}(i) \parallel^2 \\ T(\check{e}) &= \sum_{i=1}^{k} \sum_{j=1}^{2} \alpha_j \parallel \check{e}_{\phi_j}(i) \parallel^2 + \beta_j \parallel \check{e}_{p_j}(i) \parallel^2 \,, \end{cases} \tag{4}$$

with the SD least-squares residuals

$$\begin{aligned} \hat{e}_{\phi_j}(i) &= \phi_j(i) - \lambda_j \hat{a}_j - A_i \hat{b}\,, \quad \hat{e}_{p_j}(i) = p_j(i) - A_i \hat{b}\,, \\ \check{e}_{\phi_j}(i) &= \phi_j(i) - \lambda_j \check{a}_j - A_i \check{b}\,, \quad \check{e}_{p_j}(i) = p_j(i) - A_i \check{b}\,, \end{aligned}$$

and where $\parallel . \parallel^2 = (.)^T P(.)$, with P being the orthogonal projector that projects onto the range space of the DD operator D and along e_m, the m-vector having 1 at each entry. Thus when evaluated at the integer least-squares solution, the quadratic form Eq. (3) equals

$$T(\check{a}) = T(\check{e}) - T(\hat{e})\,. \tag{5}$$

This quadratic form can be evaluated once the *estimation* problem has been solved. That is, once the integer least-squares solution $\check{a}$ has been computed. The integer least-squares ambiguities are the solution to the minimization problem

$$T(\check{a}) = \min_{a} \; T(a), \quad \text{with} \;\; a \in Z^{2(m-1)}\,. \tag{6}$$

It is this minimization problem which forms the basis, either implicitly or explicitly, of all least-squares-based methods that have been proposed for computing the integer ambiguities. For a review, we refer to Teunissen (1996c). Since Eq. (6) cannot be solved as an ordinary least-squares problem, the idea is to introduce an ellipsoidal region which is based on the objective function $T(a)$. This region is known as the *ambiguity search space* and reads as

$$(\hat{a} - a)^T Q_{\hat{a}}^{-1} (\hat{a} - a) \leq \chi^2\,. \tag{7}$$

The integer least-squares estimate $\check{a}$ is then computed by means of a search within this region. The ambiguity search space is centered at $\hat{a} \in R^{2(m-1)}$, its orientation

and elongation are governed by the ambiguity variance matrix $Q_{\hat{a}}$, and its size can be controlled through χ^2.

It is the objective of the present contribution to develop the canonical form of $T(a)$, thereby giving a complete *geometric* description of the aforementioned ellipsoidal search space. Since this description should capture all intrinsic characteristics of $T(a)$, we already have from the start to face the problem of reference-satellite dependency. Let us for the moment introduce lower indices to indicate which satellite is chosen as reference when constructing the DD ambiguities. Thus the ambiguity vector a_p has satellite $p \in \{1, \ldots, m\}$ as reference and the ambiguity vector a_q has satellite $q \in \{1, \ldots, m\}$ as reference. Let the $(m-1) \times (m-1)$ matrix Z_{pq}^T, be the matrix that transforms a_q into a_p. Then

$$a_p = Z_{pq}^T a_q \ , \ \hat{a}_p = Z_{pq}^T \hat{a}_q, \ \text{ and } \ Q_{\hat{a}_p} = Z_{pq}^T Q_{\hat{a}_q} Z_{pq} \ .$$

This shows, since $Z_{pq}^T \neq I_{m-1}$ for $p \neq q$, that $a_p \neq a_q$, $\hat{a}_p \neq \hat{a}_q$ and $Q_{\hat{a}_p} \neq Q_{\hat{a}_q}$ for $p \neq q$. The quadratic form itself however, is independent of the choice of reference satellite

$$(\hat{a}_p - a_p)^T Q_{\hat{a}_p}^{-1} (\hat{a}_p - a_p) = (\hat{a}_q - a_q)^T Q_{\hat{a}_q}^{-1} (\hat{a}_q - a_q) \ .$$

This situation points out that one cannot hope to obtain a geometric description, which is invariant to the arbitrary choice of reference satellite, when one bases the analysis solely on the variance matrix of the DD ambiguities. The dilemma with which we are confronted is not unlike the one we met in *Part II* when studying the average precision of the ambiguities. There the dilemma was solved by using the idea of a double averaging. This approach does not work in the present situation however, an alternative solution has to be devised. In order to get rid of the dependence on the arbitrary choice of reference satellite, we need to go back to the reference-satellite independent generators of the DD ambiguities, which are the SD ambiguities. We therefore introduce the idea of *lifting* the DD grid into the SD space. This idea and its consequences are worked out in the next section.

3 Lifting the DD grid into the SD space

Without loss of generality, we will restrict ourselves in this section to L_1 ambiguities only. We therefore omit the index, which shows whether we are dealing with an L_1 or an L_2 ambiguity. The only indices used for the ambiguities refer to the reference satellites on which they are based. Since the DD operator is also dependent on the choice of reference satellite, it will also be given a lower index to show on which reference satellite it is based. The SD ambiguity vector will be denoted by s.

Any DD ambiguity vector a_p, $p \in \{1, \ldots, m\}$, can be parametrized as

$$a_p = \sum_{i=1}^{m-1} c_i z_i \ , \ \text{with} \ \ z_i \in Z \ , \tag{8}$$

where c_i is the canonical unit $(m-1)$-vector having 1 as its ith entry. This parametrization is in fact the description of the $(m-1)$-space of integers or of the standard grid space Z^{m-1}. The grid space Z^{m-1} lies however in R^{m-1} and not in R^m, which is the space of the SD ambiguities. Hence, it cannot be used directly to establish the link with the SD ambiguities. We therefore need to lift the stated DD grid from R^{m-1} into the SD ambiguity space R^m. In order to do so, we first need the defining relation between the SD and DD ambiguities. It reads

$$a_p = D_p^T s \ , \tag{9}$$

with the $m \times (m-1)$ matrix

$$D_p = \begin{bmatrix} I_{p-1} & 0 \\ -e_{p-1}^T & -e_{m-p}^T \\ 0 & I_{m-p} \end{bmatrix} .$$

The inverse of Eq. (9) reads

$$s = D_p (D_p^T D_p)^{-1} a_p + \mu e_m \ , \tag{10}$$

in which $D_p (D_p^T D_p)^{-1} a_p$ is a *particular* solution of Eq. (9) and μe_m the *homogeneous* part, since $D_p^T e_m = 0$. Since Eq. (10) can be seen as a parametrization of the SD ambiguities in terms of the DD ambiguities, it suggests, in analogy with Eq. (8), that the DD grid as subset of the SD ambiguity space R^m is given as

$$G_{DD} = \left\{ s \in R^m \mid s = D_p \left(D_p^T D_p \right)^{-1} a, \quad a \in Z^{m-1} \right\} . \tag{11}$$

Note that we have not taken into account the homogeneous part of Eq. (10). This is because we are primarily interested in how the DD structure propagates into R^m and not so much in its location as determined by μe_m.

It is tempting to accept Eq. (11) as *the* DD-grid in R^m. However, before this can be done, there is one point that should be taken care of first. Since matrix $D_p (D_p^T D_p)^{-1}$ in Eq. (11) depends on p and thus on the choice of reference satellite, we should first verify whether or not G_{DD} depends on this choice as well. It would not make much sense to refer to G_{DD} as the DD grid, if it still depended on the choice of reference satellite.

In order to show that G_{DD} is indeed independent of the choice for p, we will show that G_{DD} equals the orthogonal projection of the standard grid in R^m, Z^m, onto the range space of D_p. Thus

$$G_{DD} = \{ s \in R^m \mid s = P z, \quad z \in Z^m \} \ . \tag{12}$$

To prove this we need to show: if $z \in Z^m$ then $P z \in G_{DD}$ and, vice versa, if $s \in G_{DD}$ then $s = P z$ for some $z \in Z^m$. The first condition is easily verified, since $Pz = D_p (D_p^T D_p)^{-1} a$ for some $a = D_p^T z$ and $a = D_p^T z \in Z^{m-1}$ if $z \in Z^m$. In order to verify the second condition we need the following result

$$D_q^T D_p \left(D_p^T D_p \right)^{-1} = D_q^T D_p + D_q^T c_p e_{m-1}^T \ , \tag{13}$$

in which c_p is the canonical unit m-vector having 1 as its pth entry. This equation is verified as follows. From the expression for D_p in Eq. (9) follows that $D_p^T D_p = I_{m-1} + e_{m-1} e_{m-1}^T$ and thus that $(D_p^T D_p)^{-1} = I_{m-1} - e_{m-1} e_{m-1}^T / m$. This shows that $D_p (D_p^T D_p)^{-1} = D_p - e_m e_{m-1}^T / m + c_p e_{m-1}^T$. Premultiplication with D_q^T gives Eq. (13), since $D_q^T e_m = 0$. Since Eq. (13) reduces to the identity for $q = p$, we have: if $s = D_p (D_p^T D_p)^{-1} a$ for $a \in Z^{m-1}$ then $s = D_p (D_p^T D_p)^{-1} D_p^T z$ for $z = D_p a + c_p e_{m-1}^T a \in Z^m$ since $D_p^T z = a$. This verifies the second condition. The conclusion reads therefore that the grid G_{DD} as defined by Eq. (11) is indeed independent of the choice of reference satellite, despite the fact the matrix $D_p (D_p^T D_p)^{-1}$ is not.

With Eq. (12) we are now in a position to link the DD grid $G_{DD} \subset R(D_p)$ to the standard grid of the SD ambiguity space R^m. The relation between these two grids and their geometry are shown in Fig. 1. Figure 1*a* shows the orthogonal decomposition of the SD ambiguity vector $s \in R^m$ into its DD part and its homogeneous part. Figure 1*b* shows the standard grid of R^m. Figure 1*c* shows the unit box of Z^m aligned with the m-vector e_m, which itself is orthogonal to the range space $R(D_p)$. Finally, Fig. 1*d* shows the DD grid G_{DD} in $R(D_p)$. In it is also shown the projection along e_m onto $R(D_p)$ of the unit box of Fig. 1*c*.

Now that we have established the DD grid in R^m, we are also ready to position the (single-frequency) ambiguity search space in R^m. It reads

$$T(s) \leq \chi^2, \quad s \in R(D_p) \ , \tag{14}$$

with the quadratic form

$$T(s) = (\hat{s} - s)^T D_p Q_{\hat{a}_p}^{-1} D_p^T (\hat{s} - s) \ ,$$

and with $a_p = D_p^T s$, $\hat{a}_p = D_p^T \hat{s}$. Since the matrix $D_p Q_{\hat{a}_p}^{-1} D_p^T$ is guaranteed to be independent of the choice of reference satellite, we are ready to commence with our canonical analysis of the ambiguity search space. In the next section, we will first consider the single-frequency case.

4 Size, shape, and orientation of L_1 search space

In this section we will present a canonical analysis of the single-frequency ambiguity search space. The quadratic form on which it is based is given as

$$T_1 = (\hat{s}_1 - s_1)^T D Q_{\hat{a}_1}^{-1} D^T (\hat{s}_1 - s_1) \ . \tag{15}$$

Since our results are independent of the arbitrary choice of reference satellite, we have omitted the lower index denoting the reference satellite. Instead, we use a lower index to show that we are dealing with the L_1 ambiguities. The canonical decomposition of T_1 is given in the following theorem.

Theorem 1 (*Canonical form of L_1 search space*)

The single-frequency quadratic form T_1 can be written in canonical form as

$$T_1 = (\hat{s}_1 - s_1)^T R_1 \Lambda_1^+ R_1^T (\hat{s}_1 - s_1) \ ,$$

where Λ_1^+ is the pseudo-inverse of the diagonal matrix

$$\Lambda_1 = \mathrm{diag}\left(\frac{\epsilon + 1}{\alpha_1 \lambda_1^2 k} \Gamma (I_3 + \epsilon \Gamma)^{-1}, \frac{1}{\alpha_1 \lambda_1^2 k} I_{m-4}, 0 \right) \ ,$$

with: $\epsilon = \beta_1 / \alpha_1$, the L_1 phase-code variance ratio; Γ, the 3×3 diagonal matrix of gain numbers; and R_1, the $m \times m$ orthogonal matrix

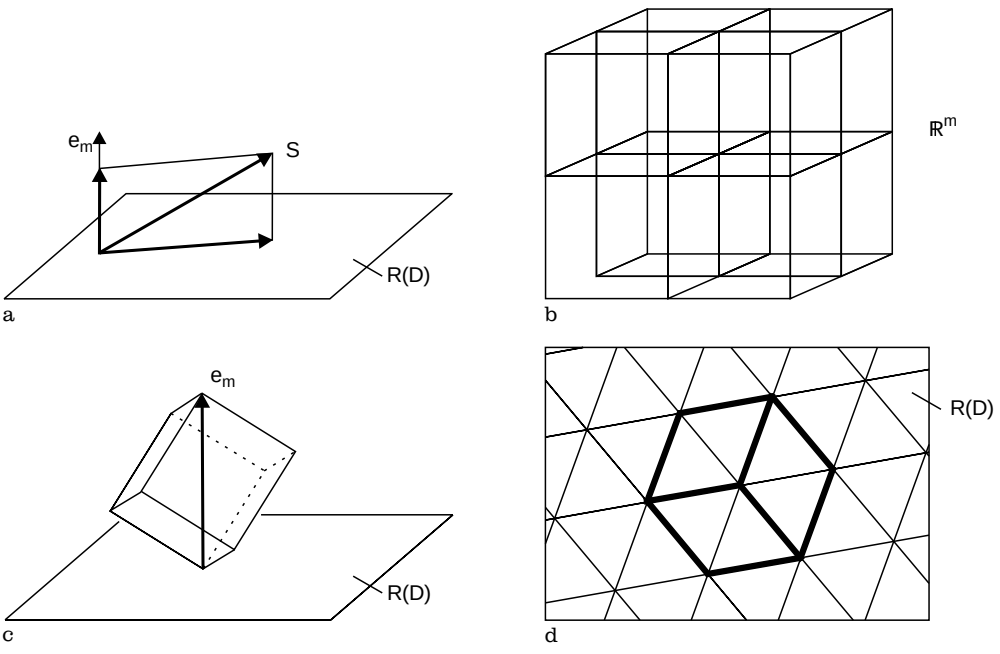

Fig. 1a–d. Geometry of $G_{DD} \subset R(D_p) \subset R^m$ and Z^m. (**a**) the orthogonal decomposition $s = D_p (D_p^T D_p)^{-1} a + \mu e_m$; (**b**) the standard grid Z^m; (**c**) the unit box of Z^m aligned with $e_m \perp R(D_p)$; (**d**) the grid $G_{DD} \subset R(D_p)$.

$$R_1 = (U, V, w)$$

with

$$\begin{cases} U = P\bar{A}F^{-T}\left(F^{-1}\bar{A}^T P\bar{A}F^{-T}\right)^{-1/2} , \\ V = E(E^T E)^{-1/2} , \\ w = e_m\left(e_m^T e_m\right)^{-1/2} , \end{cases}$$

and where E is an $m \times (m-4)$ basis matrix of the orthogonal complement of the range space of $(P\bar{A}, e_m)$.
Proof: see Appendix. □

It follows from the theorem that T_1 equals a weighted sum of squares of orthogonal projections of $(\hat{s}_1 - s_1)$ onto the orthonormal columns of U and V. If so desired, one may replace $\hat{s}_1 - s_1$ by

$$\hat{s}_1 - s_1 = D^{+T}(\hat{a}_1 - a_1) ,$$

with

$$D^{+T} = \begin{bmatrix} I_{m-1} - \frac{1}{m} e_{m-1} e_{m-1}^T \\ -\frac{1}{m} e_{m-1}^T \end{bmatrix} ,$$

where D^+ is the pseudo-inverse of the DD operator that corresponds to choosing satellite m as reference satellite.

The canonical structure as revealed by the theorem allows us to analyze the *size*, *shape*, and *orientation* of the ambiguity search space. The orientation is determined by the orthogonal matrix $R_1 = (U, V, w)$. The three orthogonal projectors that belong to the range spaces of U, V, and w are given as

$$\begin{cases} UU^T = P\bar{A}\left(\bar{A}^T P\bar{A}\right)^{-1}\bar{A}^T P , \\ VV^T = I_m - (\bar{A}, e_m)\left[(\bar{A}, e_m)^T(\bar{A}, e_m)\right]^{-1}(\bar{A}, e_m)^T , \\ ww^T = e_m\left(e_m^T e_m\right)^{-1} e_m^T = I_m - P . \end{cases} \tag{16}$$

Since they sum up to the identity matrix, their range spaces are complementary and mutually orthogonal. Hence, we have the following direct sum of R^m:

$$\begin{aligned} R^m &= R(U) \oplus R(V) \oplus R(w) \\ &= R(P\bar{A}) \oplus R(\bar{A}, e_m)^{\perp} \oplus R(e_m) . \end{aligned} \tag{17}$$

Note that the range spaces of U, V and w, but not the matrices themselves, are completely determined once $\bar{A}$, and thus the time-averaged receiver-satellite geometry, is known. Within these subspaces, the orientation of the principal axes is further determined by the matrix of gain vectors F. But as it will be shown, the orientation of the ambiguity search space is, quite remarkably, identical for the geometry-free model, the time-averaged model, and the geometry-based model.

Geometry-free model

In *Part I* it was shown how the results that hold true for the geometry-free model can be derived from the results of the geometry-based model. Hence, with $U = (u_1, u_2, u_3)$ and $V = (v_1, \ldots, v_{m-4})$, the canonical form of the geometry-free search space follows from Theorem 1 as

$$T_1 = \alpha_1 \lambda_1^2 k \frac{\epsilon}{1+\epsilon}\left\{\sum_{i=1}^{3}\left[u_i^T \Delta s_1\right]^2 + \sum_{i=1}^{m-4}\left[v_i^T \Delta s_1\right]^2\right\} , \tag{18}$$

with $\Delta s_1 = (\hat{s}_1 - s_1)$. This shows that the geometry-free search space in $R(D)$ is a perfect sphere and thus that its elongation $\tilde{e}$, as measured by the length ratio of the major and minor principal axes, equals the smallest value possible

$$\tilde{e} = 1 . \tag{19}$$

The square of the lengths of the principal axes are all equal to

$$\frac{1}{\alpha_1 \lambda_1^2 k}\left(1 + \frac{1}{\epsilon}\right) . \tag{20}$$

This shows that the size of the search space is dominated by the poor precision of the code data and that only by using a sufficient number of observation epochs (k large enough) will one be able appropriately to downsize the search space.

Time-averaged model

By taking $\gamma_i = \infty$, the result for the time-averaged model follows from Theorem 1 as

$$T_1 = \alpha_1 \lambda_1^2 k \frac{\epsilon}{1+\epsilon}\left\{\sum_{i=1}^{3}\left[u_i^T \Delta s_1\right]^2 + \frac{1+\epsilon}{\epsilon}\sum_{i=1}^{m-4}\left[v_i^T \Delta s_1\right]^2\right\} . \tag{21}$$

This shows that the orientation of the time-averaged search space is equal to that of the geometry-free search space. In fact, the two search spaces are identical in the absence of satellite redundancy ($m = 4$). In the presence of satellite redundancy however, the time-averaged search space is extended with $(m-4)$ very small principal axes. They lie in the subspace $R(V) = R(\bar{A}, e_m)^{\perp}$. Hence, in the presence of satellite redundancy the search space becomes very elongated. Its elongation is given as

$$\bar{e} = \sqrt{1 + \frac{1}{\epsilon}} . \tag{22}$$

The shape of the search space is thus independent of the receiver-satellite geometry and completely governed by the phase-code variance ratio ϵ. The elongation will get smaller when the precision of the code data improves relative to the precision of the phase data.

Geometry-based model

For the geometry-based model, the canonical decomposition reads

$$T_1 = \alpha_1 \lambda_1^2 k \frac{\epsilon}{1+\epsilon} \left\{ \sum_{i=1}^{3} \frac{1+\epsilon\gamma_i}{\epsilon\gamma_i} \left[u_i^T \Delta s_1\right]^2 + \frac{1+\epsilon}{\epsilon} \sum_{i=1}^{m-4} \left[v_i^T \Delta s_1\right]^2 \right\} . \quad (23)$$

Again we note that the orientation of the search space has remained the same. In case only one single observation epoch is used, the geometry-based search space becomes identical to the time-averaged search space. This is due to the lack of change in the receiver-satellite geometry. The two search spaces approximate each other quite well in case of very short observation time-spans. Due to the presence of the gain numbers in Eq. (23), the first three principal axes of the geometry-based search space will be shorter than their time-averaged counterparts. And they will shrink further when the change in receiver-satellite geometry increases. As to the elongation, one should discriminate between the satellite-redundant case and the nonredundant case. The elongation of the geometry-based search space is larger than that of the time-averaged search space in case satellite redundancy is absent, but smaller in case satellite redundancy is present. In the latter case, the elongation is given as

$$e = \sqrt{\frac{(1+\epsilon)\gamma_3}{1+\epsilon\gamma_3}} . \quad (24)$$

this shows, since ϵ is very small in practice and γ_3 is very large for short observation time-spans, that the ambiguity search space will still be very elongated. The elongation is much smaller, however, in the absence of satellite redundancy. In order to analyze the elongation's sensitivity with respect to the gain number γ_3 and the variance ratio ϵ, for the satellite-redundant case, we consider its partial derivatives

$$\frac{\partial e}{\partial \gamma_3} = \frac{1}{2} \sqrt{\frac{1+\epsilon}{(1+\epsilon\gamma_3)^3 \gamma_3}} , \quad \frac{\partial e}{\partial \epsilon} = -\frac{1}{2} \frac{1-1/\gamma_3}{\sqrt{(1+\epsilon)(\epsilon+1/\gamma_3)^3}} .$$

This shows that the elongation gets smaller as the maximum gain gets smaller and/or when the variance ratio gets larger. Note however, that the derivative with respect to the gain is small when the gain is large. Hence, the elongation is not very sensitive to small changes in the receiver-satellite geometry, when γ_3 is large. With respect to the variance ratio ϵ, the situation differs. Since ϵ is small in practice, the derivative is large when the gain number γ_3 is large. Hence, in case of short observation time-spans, an improvement in the precision of the code data will allow for a significant decrease in elongation.

In *Part I* it was shown how the gain in baseline precision is related to the observation time-span $(k-1)T$. This result allows us now to show the time dependency of the elongation. In order to do so, we discriminate between the phase-only case and the phase-and-code case. Using Theorem 6 of Part I, we obtain for the elongation in the phase-only case

$$e^2(\epsilon = 0) - 1 \sim \frac{1}{[(k-1)T]^2} ,$$

and when the code data are included as well, we get the relation

$$\frac{e^2(\epsilon = 0)}{e^2(\epsilon \neq 0)} - 1 \sim \frac{\epsilon}{1+\epsilon} \frac{1}{[(k-1)T]^2} .$$

This shows that the elongation is smaller when the code data are included, but also that it decreases less rapidly as function of the observation time-span than the inverse-square law which holds true for the phase-only case. Thus for a sufficiently large change in the receiver-satellite geometry, there will be no significant difference anymore between the two type of elongations.

From the preceding analysis it follows that all three types of search space have the same orientation. They only differ in the amount they are squeezed along the directions of their principal axes. Figure 2 shows the relative geometry of the three search spaces in $R(D)$ and Fig. 3 shows the geometry-based search space as a cylindrical set in R^m.

5 Size, shape, and orientation of L_1/L_2 search space

In this section we will assume that the GPS data are available on both of the frequencies L_1 and L_2. In that case, the ambiguity search space is based on the quadratic form

$$T_{12} = (\hat{s} - s)^T (I_2 \otimes D) Q_{\hat{a}}^{-1} \left(I_2 \otimes D^T\right) (\hat{s} - s) , \quad (25)$$

with the $2m$-vector of least squares SD ambiguities $\hat{s} = \left(\hat{s}_1^T, \hat{s}_2^T\right)^T$. The canonical decomposition of T_{12} is given in the following theorem.

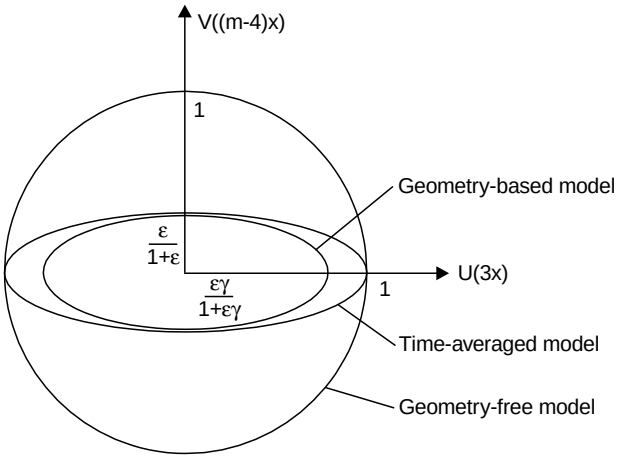

Fig. 2. The relative geometry, in $R(D)$, of the ambiguity search spaces of the geometry-free, the time-averaged, and the geometry-based model

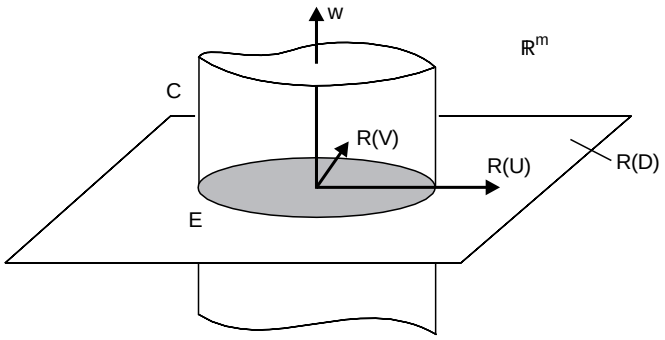

Fig. 3. The cylindrical ambiguity search space as viewed from the space of single differences, R^m

Theorem 2 (*Canonical form of L_1/L_2 search space*)

The dual-frequency quadratic form T_{12}, can be written in canonical form as

$$T_{12} = (\hat{s}-s)^T R_{12}\Lambda_{12}^{+}R_{12}^T(\hat{s}-s) \ ,$$

where Λ_{12}^{+} is the pseudo-inverse of the $2m \times 2m$ diagonal matrix

$$\Lambda_{12} = \mathrm{diag}\left(\Lambda_1, \Lambda_2, \frac{1}{\alpha_1\lambda_1^2 k} I_{m-4}, \frac{1}{\alpha_2\lambda_2^2 k} I_{m-4}, 0, 0\right) \ ,$$

and where R_{12} is the $2m \times 2m$ orthogonal matrix

$$R_{12} = \begin{bmatrix} UC & -US & V & 0 & w & 0 \\ US & UC & 0 & V & 0 & w \end{bmatrix}$$

with the diagonal matrices

$$\begin{cases} \Lambda_1 = \mathrm{diag}(\lambda_{11}, \lambda_{12}, \lambda_{13}) \ , \\ \Lambda_2 = \mathrm{diag}(\lambda_{21}, \lambda_{22}, \lambda_{23}) \ , \\ C = \mathrm{diag}(\cos(\omega_1), \cos(\omega_2), \cos(\omega_3)) \ , \\ S = \mathrm{diag}(\sin(\omega_1), \sin(\omega_2), \sin(\omega_3)) \ , \end{cases}$$

and their entries

$$\begin{cases} \lambda_{1i} = \frac{1}{(\alpha_1+\alpha_2)\lambda_1\lambda_2 k}\left[\frac{1}{2}\left(p + q\frac{(1+\epsilon)\gamma_i}{1+\epsilon\gamma_i}\right) + \frac{\gamma_i - 1}{1+\epsilon\gamma_i}\sqrt{(1+t_i^2)}\right] \ , \\ \lambda_{2i} = \frac{1}{(\alpha_1+\alpha_2)\lambda_1\lambda_2 k}\left[\frac{1}{2}\left(p + q\frac{(1+\epsilon)\gamma_i}{1+\epsilon\gamma_i}\right) - \frac{\gamma_i - 1}{1+\epsilon\gamma_i}\sqrt{(1+t_i^2)}\right] \ , \\ \sin(\omega_i) = \frac{1}{2}\sqrt{2}\left[1 - t_i \Big/ \sqrt{1+t_i^2}\right]^{1/2} \ , \quad i = 1,2,3, \end{cases}$$

with

$$\begin{cases} t_i = \frac{r(1+\epsilon\gamma_i)+s(1+\epsilon)\gamma_i}{2(\gamma_i - 1)} & \epsilon = \frac{\beta_1+\beta_2}{\alpha_1+\alpha_2} \ , \\ p = \frac{\alpha_2}{\alpha_1}\frac{\lambda_2}{\lambda_1} + \frac{\alpha_1}{\alpha_2}\frac{\lambda_1}{\lambda_2} & q = \frac{\lambda_2}{\lambda_1} + \frac{\lambda_1}{\lambda_2} \ , \\ r = \frac{\alpha_2}{\alpha_1}\frac{\lambda_2}{\lambda_1} - \frac{\alpha_1}{\alpha_2}\frac{\lambda_1}{\lambda_2} & s = \frac{\lambda_2}{\lambda_1} - \frac{\lambda_1}{\lambda_2} \ , \end{cases}$$

and where U, V and w are defined as in Theorem 1.

Proof: see Appendix. □

The canonical structure as revealed by this theorem allows us to write T_{12} as a weighted sum of squares of orthogonal projections

$$T_{12}(s_1,s_2) = T_U(s_1,s_2) + T_V(s_1,s_2) \ , \tag{26}$$

with

$$T_U(s_1,s_2) = \sum_{i=1}^{3}\frac{1}{\lambda_{1i}}\left[\cos(\omega_i)\left(u_i^T\Delta s_1\right) + \sin(\omega_i)\left(u_i^T\Delta s_2\right)\right]^2 + \sum_{i=1}^{3}\frac{1}{\lambda_{2i}}\left[-\sin(\omega_i)\left(u_i^T\Delta s_1\right) + \cos(\omega_i)\left(u_i^T\Delta s_2\right)\right]^2$$

and

$$T_V(s_1,s_2) = \alpha_1\lambda_1^2 k\sum_{i=1}^{m-4}\left(v_i^T\Delta s_1\right)^2 + \alpha_2\lambda_2^2 k\sum_{i=1}^{m-4}\left(v_i^T\Delta s_2\right)^2 \ ,$$

where $\Delta s_1 = (\hat{s}_1 - s_1)$, $\Delta s_2 = (\hat{s}_2 - s_2)$. In case of $T_V(s_1,s_2)$, the squares consist of orthogonal projections of both Δs_1 and Δs_2 onto the same orthonormal columns of V. And in case of $T_U(s_1,s_2)$, the squares consist of a double projection. Both Δs_1 and Δs_2 are first projected onto the same orthonormal columns of U, and then $\left(u_i^T\Delta s_1, u_i^T\Delta s_2\right)^T$ is projected orthogonally onto either $(\cos(\omega_i), \sin(\omega_i))^T$ or $(-\sin(\omega_i), \cos(\omega_i))^T$.

The quadratic form $T_{12}(s_1,s_2)$ should reduce to $T_1(s_1)$, in case the phase data on the second frequency are absent. Similarly, it should reduce to the single-frequency quadratic form of L_2 if the phase data on the first frequency are absent. This can be verified if we take the limits $\alpha_1 \to 0$ and $\alpha_2 \to 0$ of the eigenvalues λ_{1i}, λ_{2i} and the angle ω_i:

$$\lim_{\alpha_1\to 0}\lambda_{1i} = \infty \ , \ \lim_{\alpha_1\to 0}\lambda_{2i} = \frac{1}{\alpha_2\lambda_2^2 k}\frac{(1+\epsilon)\gamma_i}{1+\epsilon\gamma_i} \ , \ \lim_{\alpha_1\to 0}\omega_i = 0 \ ,$$

$$\lim_{\alpha_2\to 0}\lambda_{1i} = \frac{1}{\alpha_1\lambda_1^2 k}\frac{(1+\epsilon)\gamma_i}{1+\epsilon\gamma_i} \ , \ \lim_{\alpha_2\to 0}\lambda_{2i} = \infty \ , \ \lim_{\alpha_2\to 0}\omega_i = \frac{1}{2}\pi \ .$$

In order to discuss the intricacies of the canonical decomposition further, we will concentrate on some different aspects of it. First we will consider the orientation of the search space. Then we study the case where it is assumed that the gain is at its minimum or the precision of the code data is at its maximum. This is followed by the case that the gain is at its maximum or the precision of the code data is at its minimum. Finally, we will assume that the phase variance ratio α_2/α_1 equals the square of the wavelength ratio λ_1/λ_2 and see how the canonical form of the search space simplifies.

5.1 On the orientation

The ellipsoidal sets that correspond with T_{12}, T_U and T_V read

$$E_{12} = \left\{\left(s_1^T, s_2^T\right)^T \in R(I_2 \otimes D) \mid T_{12}(s_1,s_2) \le \chi^2\right\} \ ,$$

$$E_U = \left\{\left(s_1^T, s_2^T\right)^T \in R(I_2 \otimes U) \mid T_{12}(s_1,s_2) \le \chi^2\right\} \ ,$$

$$E_V = \left\{\left(s_1^T, s_2^T\right)^T \in R(I_2 \otimes V) \mid T_{12}(s_1,s_2) \le \chi^2\right\} \ .$$

The set E_{12} is the dual-frequency ambiguity search space in R^{2m}, E_U is its orthogonal projection onto $R(I_2 \otimes U)$, and E_V is its orthogonal projection onto $R(I_2 \otimes V)$. Figure 4 shows (not to scale) two-dimensional sections of E_U and E_V. The set E_V has its principal axes aligned with the v_i-axes, its shape is independent of the receiver-satellite geometry and it exists only in case satellite redundancy is present. The set E_U, on the other hand, has the orientation of its principal axes in $R(I_2 \otimes D)$ governed by ω_i, its shape is dependent on the receiver-satellite geometry, and it has a fixed dimension of 6.

As in the single-frequency case, the orthogonal matrix R_{12} is built up from the matrices U, V, and w. But in addition, we now also have the 6×6 rotation matrix

$$R = \begin{bmatrix} C & -S \\ S & C \end{bmatrix}.$$

It is determined by the three angles ω_i, $i = 1, 2, 3$. This rotation matrix reduces to the identity matrix in case the gain is at its maximum or when the code data are exact:

$$R = I_6 \Leftrightarrow \begin{cases} \gamma_i = 1, & \text{or} \\ \epsilon = \infty \end{cases} .$$

This is not likely to happen in practice though, since the code data are far from being exact and the observation time-spans will usually be short. In fact, since

$$\sin(\omega_i) = 1 \Big/ \sqrt{1 + \left(\frac{\lambda_2}{\lambda_1}\right)^2}$$

when $\gamma_i = \infty$ and $\epsilon = 0$, the angles ω_i will all be close to 38° in practice.

In order to infer the sensitivity of ω_i with respect to changes in the receiver-satellite geometry, we consider its derivative with respect to the corresponding gain number. It reads

$$\frac{\mathrm{d}\omega_i}{\mathrm{d}\gamma_i} = \sin^2(2\omega_i) \frac{(r+s)(1+\epsilon)}{4(\gamma_i - 1)^2} ,$$

from which it follows that

$$\frac{\mathrm{d}\omega_i}{\mathrm{d}\gamma_i} = 0 \Leftrightarrow \begin{cases} r = -s , \\ \epsilon = \infty , \\ \gamma_i = \infty . \end{cases}$$

This shows that the angles ω_i are rather insensitive to changes in the receiver-satellite geometry when the gain is large. A somewhat different result is obtained if we consider the sensitivity with respect to the phase-code variance ratio ϵ. For the derivative of ω_i with respect to ϵ, we get

$$\frac{\mathrm{d}\omega_i}{\mathrm{d}\epsilon} = -\sin^2(2\omega_i) \frac{(r+s)\gamma_i}{2(\gamma_i - 1)} ,$$

from which it follows that

$$\frac{\mathrm{d}\omega_i}{\mathrm{d}\epsilon} = 0 \Leftrightarrow \begin{cases} r = -s , \\ \epsilon = \infty , \\ \gamma_i = 1 . \end{cases}$$

The first condition is satisfied when the weights of the L_1 and the L_2 phase data satisfy the relation $\alpha_1 \lambda_1^2 = \alpha_2 \lambda_2^2$. This relation will later be further considered. The last two conditions ($\epsilon = \infty, \gamma_i = 1$) will generally not be satisfied in practice; instead, it is more likely that $\epsilon = 0$ and $\gamma_i = \infty$ prevails. In that case, we have

$$\frac{\mathrm{d}\omega_i}{\mathrm{d}\epsilon} = -2\frac{r+s}{q^2} ,$$

from which it follows that the derivative is about equal to -0.5 when $\alpha_1 = \alpha_2$.

The overall conclusion which we can draw from the preceding analysis is that for short observation time-spans using code data which are far less precise than the phase data, the angles ω_i will all be close to 38° and rather insensitive to changes in the receiver-satellite geometry. The angles are sensitive, though, to changes in the precision of the code data.

5.2 Minimum gain or exact code data

Having exact code data corresponds to $\epsilon = \infty$. When taking the limit $\epsilon \to \infty$ of the eigenvalues λ_{1i}, λ_{2i} and the angle ω_i, we have to discriminate between $\alpha_2 \lambda_2^2 < \alpha_1 \lambda_1^2$ and $\alpha_2 \lambda_2^2 > \alpha_1 \lambda_1^2$. The limits read

$$\lim_{\epsilon \to \infty} \lambda_{1i} = \frac{1}{\alpha_1 \lambda_1^2 k} , \quad \lim_{\epsilon \to \infty} \lambda_{2i} = \frac{1}{\alpha_2 \lambda_2^2 k} , \quad \lim_{\epsilon \to \infty} \omega_i = 0$$

if $\alpha_2 \lambda_2^2 > \alpha_1 \lambda_1^2$, and

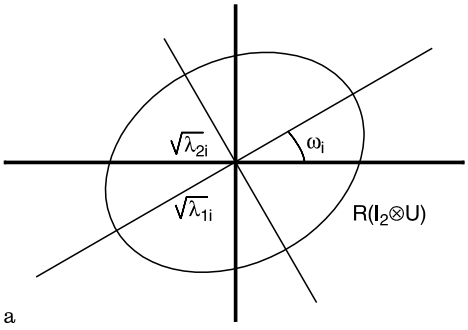

a

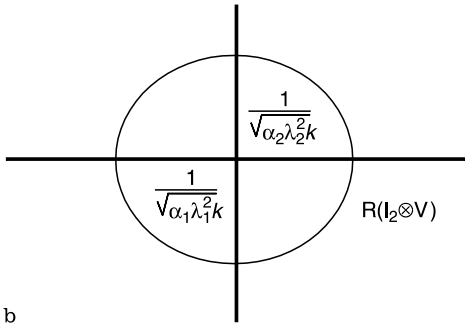

b

Fig. 4. (**a**) a 2D section of E_{12} in the subspace $R(I_2 \otimes U)$; (**b**) a 2D section of E_{12} in the subspace $R(I_2 \otimes V)$

$$\lim_{\epsilon\to\infty}\lambda_{1i}=\frac{1}{\alpha_2\lambda_2^2k}\ ,\ \lim_{\epsilon\to\infty}\lambda_{2i}=\frac{1}{\alpha_1\lambda_1^2k}\ ,\ \lim_{\epsilon\to\infty}\omega_i=\frac{1}{2}\pi$$

if $\alpha_2\lambda_2^2<\alpha_1\lambda_1^2$.

This result shows that the case of exact code data produces an ambiguity search space which is independent of the receiver-satellite geometry and of which the principal axes all have a very small length indeed. Note that both the orthogonal projections of E_{12} onto $R((D^T,0)^T)$ and $R((0,D^T)^T)$ give a perfect spheroid. The ambiguity search space E_{12} itself becomes a perfect spheroid in case of exact code data, when $\alpha_2\lambda_2^2=\alpha_1\lambda_1^2$.

This result can be understood if one considers the baseline precision. The code data can be used to solve for the baseline, without the use of the phase data. Hence, when the code data are exact, the baseline will also be exact. This implies that the phase data can be used to solve directly for the unknown ambiguities. The ambiguities will therefore directly inherit the high precision of the phase data.

The case of minimum gain ($\gamma_i=1$) will give exactly the same result as the case of exact code data. This can also be understood in terms of the baseline precision. When the gain numbers are at their minimum of 1, the variance matrix of the floated baseline becomes identical to the variance matrix of the fixed baseline. This implies that the constraining of the ambiguities, as it is done when one resolves them as integers, has no effect on the precision of the baseline. But if this is the case, the columns of the design matrix of the ambiguities in the single-baseline model must be orthogonal to the columns of the design matrix of the baseline, of course after having taking care of the respective weight matrices. Thus the normal matrix must be block diagonal and the least-squares ambiguities must be completely decorrelated from the floated baseline. But this implies that also in this case, the ambiguities directly inherit the high precision of the phase data.

5.3 Maximum gain or codeless data

In this case, we will first consider the limits $\gamma_i\to\infty$ and $\epsilon\to 0$ separately. For the case of maximum gain we have

$$\lim_{\gamma_i\to\infty}\lambda_{1i,2i}=\frac{\frac{1}{2}[(p+q)\epsilon+q]\pm\left[1+\frac{1}{4}((r+s)\epsilon+s)^2\right]^{1/2}}{(\alpha_1+\alpha_2)\lambda_1\lambda_2k\epsilon}\ , \tag{27}$$

$$\lim_{\gamma_i\to\infty}\tan(2\omega_i)=2[(r+s)\epsilon+s]^{-1}\ , \tag{28}$$

and in the case where the code data are absent, we have

$$\lim_{\epsilon\to 0}\lambda_{1i,2i}=\frac{\frac{1}{2}[(p+q)/(\gamma_i-1)+q]\pm\left[1+\frac{1}{4}((r+s)/(\gamma_i-1)+s)^2\right]^{1/2}}{(\alpha_1+\alpha_2)\lambda_1\lambda_2k/(\gamma_i-1)}\ ,$$

$$\lim_{\epsilon\to 0}\tan(2\omega_i)=2[(r+s)/(\gamma_i-1)+s]^{-1}\ .$$

Note the similarity in these two pairs of limits. The reciprocal of the phase-code variance ratio ϵ plays a similar role as (γ_i-1). It follows from these limits that

$$\lim_{\gamma_i\to\infty}\lambda_{1i}\simeq\frac{\lambda_1^2+\lambda_2^2}{(\alpha_1+\alpha_2)\lambda_1^2\lambda_2^2k\epsilon}\ ,\ \lim_{\gamma_i\to\infty}\lambda_{2i}\simeq\frac{\alpha_1+\alpha_2}{\alpha_1\alpha_2(\lambda_1^2+\lambda_2^2)k} \tag{29}$$

for ϵ small, and

$$\lim_{\epsilon\to 0}\lambda_{1i}\simeq\frac{\lambda_1^2+\lambda_2^2}{(\alpha_1+\alpha_2)\lambda_1^2\lambda_2^2k/(\gamma_i-1)}\ ,$$

$$\lim_{\epsilon\to 0}\lambda_{2i}\simeq\frac{\alpha_1+\alpha_2}{\alpha_1\alpha_2(\lambda_1^2+\lambda_2^2)k}$$

for γ_i large. This shows that the three eigenvalues λ_{1i}, $i=1,2,3$, become infinite in case the gain is at its maximum and code data are missing. In that case, the ambiguity variance matrix $Q_{\hat{a}}$ fails to exist. This can be understood as follows. An infinite gain corresponds with the use of only one single observation epoch. But if the code data are missing, a single epoch does not allow us to solve for the ambiguities on the basis of phase data only. The design matrix of the single-baseline model will have a rank defect. But since the rank defect equals only 3, there still will be $(2m-5)$ linear functions of the ambiguities that can be determined from the phase data. And the preceding result shows that these functions can be determined with a very high precision indeed. Of these functions, $2(m-4)$ correspond with the very small principal axes of E_V and the remaining three correspond with λ_{2i}, $i=1,2,3$, and thus with the three very small principal axes of E_U.

5.4 A special phase variance ratio

The canonical decomposition of T_{12} simplifies considerably if we assume that $\alpha_2/\alpha_1=\lambda_1^2/\lambda_2^2$. This follows from the limits

$$\lim_{\alpha_2\lambda_2^2\to\alpha_1\lambda_1^2}\lambda_{1i}=\frac{1}{\alpha_1\lambda_1^2k}\frac{(1+\epsilon)\gamma_i}{1+\epsilon\gamma_i}\ ,\ \lim_{\alpha_2\lambda_2^2\to\alpha_1\lambda_1^2}\lambda_{2i}=\frac{1}{\alpha_1\lambda_1^2k}\ , \tag{30}$$

and

$$\lim_{\alpha_2\lambda_2^2\to\alpha_1\lambda_1^2}\tan(2\omega_i)=2\left(\frac{\lambda_2}{\lambda_1}-\frac{\lambda_1}{\lambda_2}\right)^{-1}.$$

Hence in this case, E_V is a perfect spheroid of dimension $2(m-4)$ and E_U is a six-dimensional ellipsoid with an elongation which is identical to the elongation of E_{12}, which in turn is identical to the elongation of E_1. Thus both E_U and E_{12} will be extremely elongated when the maximum gain number γ_3 is large and the phase-code variance ratio ϵ is small. Note that although the shape of E_U is dependent on the receiver-satellite geometry, its

orientation in $R(I_2 \otimes D)$ is not. In fact, ω_i is independent of both the gain numbers γ_i and the phase-code variance ratio ϵ. All three angles ω_i, $i = 1, 2, 3$, are identical and about equal to 38°.

The preceding result also allows an easy comparison to be made with the results of Theorem 1, discriminating between the impacts of the three different GPS models. For an easy reference, we have summarized these results in Fig. 5. The Λ-matrices contain the squares of the lengths of the principal axes. Their index shows their order. The figure shows for the geometry-free model, the time-averaged model, and the geometry-based model, how the lengths of the principal axes are built up from the common scale factor

$$\frac{1}{\alpha_1 \lambda_1^2 k}\left(1+\frac{1}{\epsilon}\right) ,$$

and by how much the principal axes get squeezed when additional information is used. It clearly shows the contributions of dual-frequency data, of satellite redundancy, and of the receiver-satellite geometry in reducing the lengths of the principal axes. The lower line is absent in case only single-frequency data are used and the middle line is absent in case satellite redundancy is absent.

6 Ambiguity search halting

In the previous two sections we have studied the intrinsic geometry of the ambiguity search space. This was done for the geometry-free model, the time-averaged model, and the geometry-based model. In this section we will show how the elongated shape of the ambiguity search space effects the actual computation of the integer least-squares ambiguities. This allows us to explain the behavior of search halting which is typically experienced when one computes DD integer ambiguities. We will also show what impact the widelane transformation has on the shape of the ambiguity search space and on the search of the ambiguities. As a result it will become clear that one can do much better than the widelane ambiguities, even within the rather restricted class of ambiguity transformations that fail to take the receiver-satellite geometry into account. Ultimately however, the strongest decorrelation is achieved when the ambiguity transformation is multivariate instead of only two dimensional and when it is constructed from using the available information on the receiver-satellite geometry.

6.1 Partial search spaces

The computation of the integer least-squares ambiguities is based on a search inside the ambiguity search space

$$(\hat{a}-a)^T Q_{\hat{a}}^{-1}(\hat{a}-a) \leq \chi^2 . \tag{31}$$

In order to formulate the bounds on which the search is based, a *sequential conditional least-squares adjustment* is carried out, thus allowing the quadratic form Eq. (31) to be written as a sum of independent squares. As a result, scalar bounds on the individual ambiguities can be formulated, which are then used in the sequential search for the sought for integer ambiguities. For our present purposes, we do not need the complete factorization into a sum of independent scalar squares. It suffices to factorize Eq. (31) into a sum of two independent quadratic forms. We therefore partition the ambiguity vector as $a = \left(a_1^T, a_2^T\right)^T$. Its variance matrix is partitioned accordingly. The least-squares estimator of a_2, *conditioned* on a_1, then reads

$$\hat{a}_{2|1} = \hat{a}_2 - Q_{21}Q_{11}^{-1}(\hat{a}_1 - a_1) . \tag{32}$$

This ambiguity estimator is not correlated with $\hat{a}_1$ and its variance matrix is given as

$$Q_{22|1} = Q_{22} - Q_{21}Q_{11}^{-1}Q_{12} . \tag{33}$$

Since $\hat{a}_{2|1}$ is not correlated with $\hat{a}_1$, we can write the quadratic form of Eq. (31) as a sum of two quadratic forms, in $\hat{a}_1$ and $\hat{a}_{2|1}$, respectively. As a result, the ambiguity search space can also be formulated by means of the two inequalities

$$\begin{cases} (\hat{a}_1 - a_1)^T Q_{11}^{-1}(\hat{a}_1 - a_1) & \leq \chi^2 , \\ (\hat{a}_{2|1} - a_2)^T Q_{22|1}^{-1}(\hat{a}_{2|1} - a_2) & \leq \chi_1^2 , \end{cases} \tag{34}$$

where $\chi_1^2 = \chi^2 - (\hat{a}_1 - a_1)^T Q_{11}^{-1}(\hat{a}_1 - a_1)$. Were one to continue this factorization to the level of the individual ambiguities, one would obtain the set of scalar bounds on the individual ambiguities which are used in the search.

The two inequalities of Eq. (34) can be interpreted as a decomposition of the ambiguity search space Eq. (31) into two *partial* ambiguity search spaces, one for the partial ambiguity vector a_1 and one for the partial ambiguity vector a_2. The first of these partial ambiguity search spaces is centered at $\hat{a}_1$, its size is controlled by χ^2 and its shape governed by Q_{11}. The second is centered at $\hat{a}_{2|1}$, with its size controlled by χ_1^2 and its shape governed by $Q_{22|1}$. Since $\hat{a}_{2|1}$ depends on a_1, also the location and

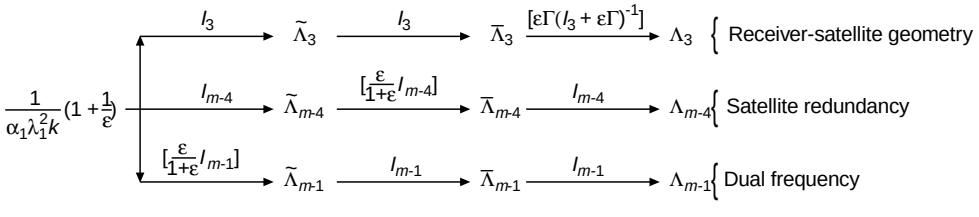

Fig. 5. Shrinkage of ambiguity principal axes for the geometry-free model ($\tilde{\Lambda}$), the time average model ($\bar{\Lambda}$) and the geometry-based model (Λ). For the dual-frequency case it has been assumed that $\alpha_1\lambda_1^2 = \alpha_2\lambda_2^2$

size of the second partial search space depend on it. Its shape however, is independent of it.

It will be clear that the characteristics of the variance matrix $Q_{\hat{a}}$ and thus also those of the variance matrices Q_{11} and $Q_{22|1}$, to a large extent influence the efficiency with which the search can be performed. The search becomes trivial for instance, when all ambiguities would be uncorrelated. In that case the sought-for integer least-squares ambiguities simply follow from rounding the least-squares ambiguities to their nearest integer. The search is nontrivial however, when the ambiguities are correlated. In fact, the search becomes rather time consuming when the ambiguities are heavily correlated. To see this, assume that $\hat{a}_1$ and $\hat{a}_2$ are highly correlated. Conditioning on a_1 will then result in a greatly improved precision for the second set of ambiguities. This implies, assuming that the ambiguities are all of about the same precision, that the conditional variance matrix $Q_{22|1}$ will be much 'smaller' than the unconditional variance matrix Q_{11}. Hence

$$Q_{22|1} \ll Q_{11} \ . \tag{35}$$

But this implies that the second partial search space of Eq. (34) would be very much smaller than the first. As a consequence *search halting* will be experienced. That is, for many of the integer vectors a_1 that satisfy the first inequality of Eq. (34), no corresponding integer vectors a_2 can be found that satisfy the second inequality. Thus many of the integer candidates a_1, which looked promising based on the first inequality, would then have been computed without avail.

The phenomenon of search halting as just described is precisely what happens when the search is based on the DD ambiguities. With the results of the previous two sections we are now in a position to show this. We will only show it for the single-frequency case. For the dual-frequency case it can be shown in a similar way.

Since the variance matrix of the L_1 DD ambiguities is given as $Q_{\hat{a}} = D^T(R_1\Lambda_1^+R_1)^+D$, it follows from Theorem 1 that

$$\begin{aligned} Q_{\hat{a}} &= \frac{1}{\alpha_1\lambda_1^2 k} D^T\Big[U(1+\epsilon)\Gamma(I_3+\epsilon\Gamma)^{-1}U^T + WW^T\Big]D \\ &= \frac{1}{\alpha_1\lambda_1^2 k} D^T\Big[I_m + U(\Gamma - I_3)(I_3+\epsilon\Gamma)^{-1}U^T\Big]D \ . \end{aligned} \tag{36}$$

The first equality follows from the theorem, the second follows since $D^Tw = 0$ and since the three orthogonal projectors UU^T, WW^T, and ww^T sum to the identity matrix.

Since ϵ is small and γ_i very much larger than 2 for short observation time-spans, it follows that

$$\gamma_i \gg \frac{2}{1-\epsilon} \ . \tag{37}$$

This implies that the entries of the second matrix within the square brackets of the second equation of Eq. (36), can be expected to be very much larger than the entries of the first matrix within these square brackets, the entries of the identity matrix. Hence, if we partition matrix D as $D = (D_1, D_2)$, we have to a good approximation

$$Q_{11} \simeq \frac{1}{\alpha_1\lambda_1^2 k} D_1^T\Big[U(\Gamma - I_3)(I_3+\epsilon\Gamma)^{-1}U^T\Big]D_1 \ ; \tag{38}$$

and a similar approximation can be given for Q_{12} and Q_{22}. If we now assume that the 3×3 matrix D_1^TU is invertible, it follows upon substituting the approximations for Q_{11} and Q_{12} into Eq. (33) that $Q_{22|1}$ can be approximated as

$$Q_{22|1} \simeq \frac{1}{\alpha_1\lambda_1^2 k} D_2^TD_2 \ . \tag{39}$$

Comparing this conditional variance matrix with the unconditional variance matrix Eq. (38) shows, since Eq. (37) holds true, that the inequality Eq. (35) is indeed satisfied. The conditional variances of the last $(m-4)$ ambiguities are thus very much smaller than the variances of the first three ambiguities. In fact, the conditional variances of the last $(m-4)$ ambiguities are governed by the high precision of the phase data, whereas when the gain numbers are sufficiently large, the variances of the first three ambiguities are governed by the poor precision of the code data. Also note that for the approximation used, the conditional variance matrix is independent of the receiver-satellite geometry. It only varies when the number of observation epochs varies. For two epochs and a standard deviation of 0.3 cm for the SD phase data, the conditional standard deviations of the last $(m-4)$ ambiguities are all of about the order of 0.02 of a cycle. This is indeed the order one will typically find in practice.

From the preceding analysis we can conclude that the search halting which is experienced when solving for the integer DD ambiguities is due to the highly elongated shape of the ambiguity search space. In case of the time-averaged model and the geometry-based model, the search space has three very long principal axes, while the remaining principal axes are very short. This is true for the single-frequency case and for the dual-frequency case. Hence, the three long principal axes mainly govern Q_{11}, whereas the very small principal axes govern $Q_{22|1}$. As a result, search halting is experienced when passing from the third to the fourth bound in the sequentially conditional least-squares-based search.

In case of the geometry-free model we have a somewhat different result. In the dual-frequency case, there are now $(m-1)$ very long principal axes and an equal number of very short principal axes. Hence, in this case the search halting will take place when passing from the $(m-1)$th bound to the mth bound. In the single-frequency case, there are no differences in the lengths of the principal axes. This implies that no search halting is expected to take place for this particular case.

The fact that one will not have any difficulties in computing the integer least-squares estimates of the DD ambiguities when using the single-frequency geometry-

free model, does *not* imply of course that this model should be preferred over the other models. Here it is important to make a clear distinction between the integer *estimation* problem and the integer *validation* problem. The phenomenon of search halting is met when solving the integer estimation problem in terms of DD ambiguities. It is a *computational* inconvenience, which although serious, does not imply that 'poorer' estimates are computed when it occurs. Quite the contrary in fact. The large disparity in the lengths of the principal axes is very beneficial for the validation of the integer estimates, in the sense that it very much helps to improve the quality of the integer least-squares solution. This will be shown and discussed in detail in *Part IV*.

From this discussion it will be clear that in order to lessen the computational burden of finding the integer least-squares solution, we need a way to get rid of the problem of search halting. In the next subsection, we will investigate what the widelane ambiguity has to offer in this respect.

6.2 The widelane transformation

In *Part II* the impact on the precision and correlation of the ambiguities of using the widelane transformation was analyzed. It was shown that it is not guaranteed that the introduction of the widelane ambiguities improves the precision of the ambiguities. As to whether or not it improves the precision depends first of all on the type of model used (geometry-free, time-averaged, or geometry-based). In case of the geometry-free model it always improves the precision. In case of the time-averaged and geometry-based model however, it depends on the strength of the receiver-satellite geometry, on the presence or absence of satellite redundancy and on the relative precision of the phase and code data. It was shown for circumstances which are typically experienced in practice, that the introduction of the widelane ambiguities improves by a factor of about 20 the precision of those three ambiguity functions that have the poorest precision, while it degrades by a factor of about 1.61 the precision of the remaining ambiguity functions, which are those with the best possible precision.

Also the conditions for the widelane transformation to decorrelate the ambiguities were derived. Here we saw a similar mechanism at work as that which we saw when studying the precision. That is, ambiguity functions that are highly correlated get decorrelated, while those which are already decorrelated get somewhat correlated.

In the present subsection we will show how the widelane transformation affects the shape of the ambiguity search space. As a consequence, it allows us to study its impact on the search for the integer least-squares ambiguities. Since we know, from Theorem 1, how the canonical form of the search space looks for the geometry-based model, and since we also know how to obtain from it the corresponding canonical forms for the time-averaged model and the geometry-free model, we can study the impact of the widelane transformation for the three models together.

The matrix $Q_{\hat{a}} = (I_2 \otimes D^T)\big(R_{12}\Lambda_{12}^{+}R_{12}^T\big)^{+}(I_2 \otimes D)$ is the dual-frequency variance matrix of the DD ambiguities for the geometry-based model. Using Theorem 2, it can be written as

$$\begin{aligned} Q_{\hat{a}} = {} & \big(I_2 \otimes D^T U\big)\Sigma_{\hat{a}}\big(I_2 \otimes U^T D\big) \\ & + \big(I_2 \otimes D^T V\big)\Omega_{\hat{a}}\big(I_2 \otimes V^T D\big)\ , \end{aligned} \tag{40}$$

with

$$\Sigma_{\hat{a}} = \begin{bmatrix} C & -S \\ S & C \end{bmatrix}\begin{bmatrix} \Lambda_1 & 0 \\ 0 & \Lambda_2 \end{bmatrix}\begin{bmatrix} C & S \\ -S & C \end{bmatrix},$$

$$\Omega_{\hat{a}} = \begin{bmatrix} \frac{1}{\alpha_1\lambda_1^2 k} I_{m-4} & 0 \\ 0 & \frac{1}{\alpha_2\lambda_2^2 k} I_{m-4} \end{bmatrix}.$$

Matrix $\Sigma_{\hat{a}}$ is of order six and the diagonal matrix $\Omega_{\hat{a}}$ is of order $2(m-4)$. The only nonzero entries of matrix $\Sigma_{\hat{a}}$ are on its main diagonal and on two subdiagonals.

In order to obtain the corresponding decomposition for the time-averaged model, we simply have to replace $\Sigma_{\hat{a}}$ in Eq. (40) by

$$\Sigma_{\bar{a}} = \Sigma \otimes I_3\ ,$$

where

$$\Sigma = \begin{bmatrix} c & -s \\ s & c \end{bmatrix}\begin{bmatrix} \lambda_1 & 0 \\ 0 & \lambda_2 \end{bmatrix}\begin{bmatrix} c & s \\ -s & c \end{bmatrix},$$

with its entries given by the limits

$$\left.\begin{matrix} \lambda_1 \\ \lambda_2 \\ \omega \end{matrix}\right\} = \lim_{\gamma_i \to \infty} \left\{\begin{matrix} \lambda_{1i} \\ \lambda_{2i} \\ \omega_i \end{matrix}\right.$$

These limits are given in Eqs. (27) and (28).

In order to obtain the corresponding decomposition for the geometry-free model, we need in addition to the replacement of the last paragraph, to replace $\Omega_{\hat{a}}$ in Eq. (40) by

$$\Omega_{\bar{a}} = \Sigma \otimes I_{m-4}\ .$$

We are now in a position to apply the widelane transformation. The widelane transformation is given as $Z_w^T \otimes I_{m-1}$, with

$$Z_w^T = \begin{bmatrix} 1 & -1 \\ 0 & 1 \end{bmatrix}. \tag{41}$$

After the widelane transformation has been applied, the geometry-based ambiguity variance matrix reads $Q_{\hat{w}} = \big(Z_w^T \otimes I_{m-1}\big)Q_{\hat{a}}\big(Z_w \otimes I_{m-1}\big)$. Since $Z_w^T \otimes I_{m-1}$ commutes with $[I_2 \otimes (D^T U, D^T V)]$, the variance matrix $Q_{\hat{w}}$ follows from Eq. (40) as

$$\begin{aligned} Q_{\hat{w}} = {} & \big(I_2 \otimes D^T U\big)\Sigma_{\hat{w}}\big(I_2 \otimes U^T D\big) \\ & + \big(I_2 \otimes D^T V\big)\Omega_{\hat{w}}\big(I_2 \otimes V^T D\big), \end{aligned} \tag{42}$$

with

$$\Sigma_{\hat{w}} = \left(Z_w^T \otimes I_3\right)\Sigma_{\hat{a}}(Z_w \otimes I_3),$$
$$\Omega_{\hat{w}} = \left(Z_w^T \otimes I_{m-4}\right)\Omega_{\hat{a}}(Z_w \otimes I_{m-4}) \ .$$

For the time-averaged model and the geometry-free model, the corresponding results follow if we make the appropriate substitutions for $\Sigma_{\hat{a}}$ and $\Omega_{\hat{a}}$.

Based on these results, some interesting observations can be made. First, note that when comparing Eq. (42) with Eq. (40), the widelane transformation only affects the two matrices $\Sigma_{\hat{a}}$ and $\Omega_{\hat{a}}$. This implies that once the eigenvalue-eigenvector structures of $\Sigma_{\hat{w}}$ and $\Omega_{\hat{w}}$ are known, the dual-frequency variance matrix $Q_{\hat{w}}$ can be given a canonical decomposition which is very similar to the one given in Theorem 2. Also note that the eigenvalue-eigenvector structures of $\Sigma_{\hat{w}}$ and $\Omega_{\hat{w}}$ are not too difficult to derive. Due to its structure, the 6×6 matrix $\Sigma_{\hat{w}}$ can be decoupled into three 2×2 matrices. And the $2(m-4) \times 2(m-4)$ matrix $\Omega_{\hat{w}}$ can be decoupled into $(m-4)$ identical 2×2 matrices. Thus in total, only four 2×2 matrices need to be handled in case of the geometry-based model. For the other two models it is even less. For the time-averaged model, it will be two 2×2 matrices and for the geometry-free model only one such matrix. Once their eigenvalue-eigenvector structures are given, a complete canonical decomposition of the widelane-based search space is available.

For our present purposes, we do not need the complete canonical decomposition of $Q_{\hat{w}}$. It suffices to restrict our attention to the lengths of the principal axes. We will therefore concentrate on the eigenvalues of $\Sigma_{\hat{a}}$, $\Omega_{\hat{a}}$ and of $\Sigma_{\hat{w}}$, $\Omega_{\hat{w}}$. First we will consider the eigenvalues of the three pairs of 2×2 matrices that are captured in $\Sigma_{\hat{a}}$ and $\Sigma_{\hat{w}}$.

We know that $\Lambda_1 >> \Lambda_2$ and thus that $\lambda_{1i} >> \lambda_{i2}$, for $i = 1, 2, 3$. We also know that the widelane transformation Eq. (41) is area preserving and that it is likely to decorrelate. From these last two properties it follows that for the two-dimensional case, the widelane transformation forces the ellipse to become more circular-like. Hence, if we denote the eigenvalues *after* the widelane transformation has been applied as μ_{1i} and μ_{2i}, it follows that the inequality

$$\frac{\lambda_{1i}}{\lambda_{2i}} > \frac{\mu_{1i}}{\mu_{2i}} \tag{43}$$

must hold. The question now is, how much smaller is the second ratio when compared to the first ratio? In the ideal case, we would of course like the second ratio to be identical to 1. In that case the corresponding lengths of the six principal axes would all become equal, with the result that they would no longer be responsible for the phenomenon of search halting.

In order to analyze Eq. (43), we will assume that the phase data are equally precise ($\alpha_1 = \alpha_2 = \alpha$) and that the observation time-span is such that we may use the approximation $\gamma_i \to \infty$. According to Eq. (29), the eigenvalues of $\Sigma_{\hat{a}}$ and of $\Sigma_{\check{a}}$, are then approximately given as

$$\lambda_{1i} \simeq \frac{\lambda_1^2 + \lambda_2^2}{2\alpha\lambda_1^2\lambda_2^2 k\epsilon} \ , \ \lambda_{2i} \simeq \frac{2}{\alpha\left(\lambda_1^2 + \lambda_2^2\right)k} \ . \tag{44}$$

In a similar way we can derive the eigenvalues after the widelane transformation has been applied. This gives then the approximation

$$\mu_{1i} \simeq \frac{\lambda_1^2 + (\lambda_1 - \lambda_2)^2}{2\alpha\lambda_1^2\lambda_2^2 k\epsilon} \ , \ \mu_{2i} \simeq \frac{2}{\alpha\left(\lambda_1^2 + (\lambda_1 - \lambda_2)^2\right)k} \ . \tag{45}$$

Note that $\lambda_{1i}\lambda_{2i} = \mu_{1i}\mu_{2i}$. This reflects the area-preserving property of the widelane transformation. If we now take the ratios of the eigenvalues, it follows from Eqs. (44) and (45) that

$$\frac{\lambda_{1i}}{\lambda_{2i}} \simeq \frac{1}{4}\left[\frac{\lambda_1}{\lambda_2} + \frac{\lambda_2}{\lambda_1}\right]^2 \frac{1}{\epsilon} \ , \ \frac{\mu_{1i}}{\mu_{2i}} \simeq \frac{1}{4}\left[\frac{\lambda_1}{\lambda_2} + \frac{\lambda_2}{\lambda_1}\left(1 - \frac{\lambda_1}{\lambda_2}\right)^2\right]^2 \frac{1}{\epsilon} \ . \tag{46}$$

This shows that inequality Eq. (43) is indeed fulfilled. But it also shows that the second ratio is still far from being close to 1. For $\epsilon = 10^{-4}$, the first ratio is about equal to 103^2, while the second is about equal to 42^2.

This change in the eigenvalues holds true for all three models. However, when satellite redundancy is present ($m > 4$), we also need to consider for both the geometry-based model as well as for the time-averaged model what happens to $\Omega_{\hat{a}}$. Since the two matrices of $\Omega_{\hat{a}}$ on which the widelane transformation operates are already diagonal, the situation cannot improve, but instead only get worse. That is, the differences between the eigenvalues will get larger instead of smaller. Fortunately, since both $1/\alpha_1\lambda_1^2 k$ and $1/\alpha_2\lambda_2^2 k$ are very small, also the eigenvalues of $\Omega_{\hat{w}}$ and their differences will remain suffiently small. Hence for all practical purposes, no significant change in the impact on the search can be expected from this small change in eigenvalues.

The overall conclusion from this analysis is that the widelane transformation indeed succeeds in pushing the three, or in the case of the geometry-free model, the $(m-1)$ very large eigenvalues down to smaller values and pulling the three or $(m-1)$ small eigenvalues up to larger values. For the search of the integer least-squares solution this has two favourable consequences. First, since the large eigenvalues get smaller, the first partial ambiguity search space of Eq. (34) will get smaller, thus allowing a smaller number of integer candidates. Second, since the *gap* between the large eigenvalues and the following small eigenvalues is made smaller as well, the difference between Q_{11} and $Q_{22|1}$ becomes less pronounced as before, which implies that less search halting will take place.

Although the widelane transformation does improve the situation, we have already remarked that there seems to be considerable room for further improvement. In the next subsection we will show that one can indeed do much better than the widelane transformation.

6.3 On decorrelating transformations

When constructing the decomposition Eq. (42) of the variance matrix $Q_{\hat{w}}$, we observed that the widelane transformation $Z_w^T \otimes I_{m-1}$ commuted with the matrix $[I_2 \otimes (D^T U, D^T V)]$. But this property is *not* unique for the widelane transformation. There is a whole class of transformations which have this property. Every $2(m-1) \times 2(m-1)$ matrix that can be written as $Z^T \otimes I_{m-1}$ has this property. Thus, as long as this matrix is an admissible ambiguity transformation, one can analyze in exactly the same way as was done in the previous subsection its impact on the shape of the ambiguity search space. The transformation is admissible when the matrix

$$Z^T = \begin{bmatrix} z_{11} & z_{12} \\ z_{21} & z_{22} \end{bmatrix} \tag{47}$$

is area preserving and its entries are all integers. After applying the transformation, the variance matrix of the transformed ambiguities becomes

$$\begin{aligned} Q_{\hat{z}} = &\left(I_2 \otimes D^T U\right) \Sigma_{\hat{z}} \left(I_2 \otimes U^T D\right) \\ &+ \left(I_2 \otimes D^T V\right) \Omega_{\hat{z}} \left(I_2 \otimes V^T D\right) , \end{aligned} \tag{48}$$

where $\Sigma_{\hat{z}}$ and $\Omega_{\hat{z}}$ play the same role as the two matrices $\Sigma_{\hat{w}}$ and $\Omega_{\hat{w}}$ of Eq. (42). With this result we are now in a position to develop ambiguity transformations of the form of Eq. (47), which do a better job in appropriately molding the shape of the ambiguity search space than the widelane transformation does. Some examples are given in Table 1, for different values of ϵ. It shows, for instance for $\epsilon = 10^{-4}$, that the transformation

$$Z^T = \begin{bmatrix} -3 & 4 \\ -4 & 5 \end{bmatrix}$$

reduces the eigenvalue ratio from $(103)^2$ to $(1.6)^2$ as opposed to the value $(42)^2$, which we had earlier with the widelane transformation.

The transformations of Table 1 are optimal for the geometry-free model. Although better than the widelane transformation, these transformations are still not optimal, however, for the time-averaged model and the geometry-based model. The reason for this is the following. First, they require that dual-frequency data are available. Second, they fail to take the existing relative receiver-satellite geometry into account. It is precisely due to these two restrictions that the transformed ambiguity variance matrix Eq. (48) takes on a form which resembles that of the original DD ambiguity variance matrix. There is no interaction between the $\Sigma_{\hat{z}}$ matrix and the $\Omega_{\hat{z}}$ matrix. Also, the two semi-orthogonal matrices U and V, in which the receiver-satellite geometry is predominantly present, stay untouched by the transformation. Much more leeway in improving the shape of the ambiguity search space is available however, when the dual-frequency DD ambiguity variance matrix is transformed by a $2(m-1) \times 2(m-1)$ matrix of which still *all* the entries can be appropriately selected, as opposed to only the four of $Z^T \otimes I_{m-1}$. This is the approach taken with the LAMBDA method. Since it is not bound by the afore mentioned restrictions, it allows one to take the existing receiver-satellite geometry into account, and it works both for the single-frequency case as well as for the dual-frequency case. Typical results that can be obtained with the method are reported in Teunissen (1994), de Jonge and Tiberius (1995), and Tiberius and de Jonge (1995).

Table 1. 2D decorrelating ambiguity transformations and their effect on elongation ($e_L \rightarrow e_z$) compared with the widelane elongation (e_w)

ϵ ($\gamma_i = \infty$)	e_L	e_w	Z^T	e_z
0.25×10^{-4}	206	84	$\begin{bmatrix} -7 & 9 \\ -4 & 5 \end{bmatrix}$	1.6
10^{-4}	103	42	$\begin{bmatrix} -3 & 4 \\ -4 & 5 \end{bmatrix}$	1.6
9×10^{-4}	34	14	$\begin{bmatrix} -3 & 4 \\ 1 & -1 \end{bmatrix}$	1.4

7 Summary

In this contribution we studied the geometry of the ambiguity search space. Canonical forms were derived for the single-frequency and the dual-frequency search spaces of the geometry-based model, the time-averaged model, and the geometry-free model. It was shown that the orientation of the single-frequency search space is identical for all of the three models. The three search spaces only differ in the lengths of their principal axes. These differences however, can be very significant. It was shown how and to what extent the shape of the search space alters when the gain numbers, the phase-code variance ratio, or the satellite redundancy change. The single-frequency search space of the time-averaged model coincides with that of the geometry-free model in case satellite redundancy is absent, and it coincides with the search space of the geometry-based model when in addition to the absence of satellite redundancy, the gain numbers tend to infinity.

The canonical form of the dual-frequency search space is somewhat more intricate than its single-frequency counterpart. In particular an additional rotation enters due to the inclusion of the second frequency. This rotation is the multivariate generalization of that which we already met in *Part II*. The three angles of rotation depend on the observation weights and on the gain-numbers. Their dependency on the receiver-satellite geometry make the orientation of the dual-frequency search space differ for the three single-baseline models. This difference will be small however when the gain numbers are large. The principal axes of the search space can be divided into two sets according to their length. For the geometry-free model, there are $(m-1)$ principal axes which have a very small length, and an equal number which have a very large length. For the time-averaged model, the number of short principal axes

has increased by $(m-4)$ to $(2m-5)$. Thus in this case there are only three long principal axes. The same holds true for the geometry-based model, even though they are smaller than their counterparts of the time-averaged model.

We also explained the phenomenon of search halting which is typically experienced when one performs the search for the integer least-squares solution of the DD ambiguities. Based on the canonical forms of the search spaces, one can predict if and at what level of the search the search halting will occur. Using the widelane transformation as an example, it was shown how decorrelating ambiguity transformations permit one to mold the shape of the search space, such that the computational burden of the integer search is lessened. But it was also shown that if one uses ambiguity transformations that are optimized with respect to the decorrelation property, one can generally do much better than the widelane transformation.

Appendix

Proof of Theorem 1 (*Canonical form of L_1 search space*) According to Theorem 1 of *Part II*, the variance matrix of the L_1 ambiguities is given as

$$Q_{\hat{a}_1} = \frac{1}{\lambda_1^2}\left[\frac{1}{\alpha_1 k} D^T D + D^T \bar{A} Q_{\hat{b}}(\phi,p) \bar{A}^T D\right] . \tag{49}$$

Inversion, premultiplication with D and postmultiplication with D^T, gives

$$D Q_{\hat{a}_1}^{-1} D^T = \alpha_1 \lambda_1^2 k \left[P - \alpha_1 k P \bar{A} Q_{\hat{b}}(\phi,p) \bar{A}^T P\right] . \tag{50}$$

Note that $Q_{\hat{a}_1}$ is expressed in the variance matrix of the floated baseline, whereas $D Q_{\hat{a}_1}^{-1} D^T$ is expressed in the variance matrix of the fixed baseline.

In order to construct the canonical form of Eq. (49), we need to solve the eigenvalue problem

$$\alpha_1 \lambda_1^2 k \left[P - \alpha_1 k P \bar{A} Q_{\hat{b}}(\phi,p) \bar{A}^T P\right] x = \lambda x . \tag{51}$$

We will solve this eigenvalue problem in three steps. *First step*: since matrix $D Q_{\hat{a}_1}^{-1} D^T$ has a rank defect of 1, it has one zero eigenvalue. The corresponding eigenvector lies in the null space $N(D^T)$ and is thus given by $x = e_m$. The normalized eigenvector and its eigenvalue read therefore

$$w = e_m \left(e_m^T e_m\right)^{-1/2} , \quad \lambda = 0 . \tag{52}$$

Second step: due to the orthogonality of the eigenvectors, the remaining eigenvectors satisfy $x \in R(e_m)^{\perp} = R(D)$. Hence, for the remaining eigenvectors we have $Px = x$. This shows, together with Eq. (51), that if x lies in the null space $N\left(\bar{A}^T P\right)$, then x is an eigenvector having the eigenvalue $\alpha_1 \lambda_1^2 k$. In order to find out how many of these eigenvectors exist, we need to know the dimension of the intersection $R(D) \cap N\left(\bar{A}^T P\right)$. Since $\dim R(D) = m-1$ and $\dim N\left(\bar{A}^T P\right) = m-3$, the dimension of the intersection is less than or at the most equal to $(m-3)$. Since $x \in R(D) \cap N\left(\bar{A}^T P\right)$ is equivalent to $\bar{A}^T P x = 0$ and $x = Dy$ for some $y \in R^{m-1}$, it is also equivalent to $\bar{A}^T D y = 0$ and $x = Dy$ for some $y \in R^{m-1}$. This shows that the dimension of $R(D) \cap N\left(\bar{A}^T P\right)$ equals the dimension of the null space $N\left(\bar{A}^T D\right)$, which is $(m-4)$. Hence, there exist $(m-4)$ linear independent eigenvectors having the eigenvalue $\alpha_1 \lambda_1^2 k$. If we introduce an $m \times (m-4)$ basis matrix E of $R(D) \cap N\left(\bar{A}^T P\right)$, the matrix of orthonormal eigenvectors and the corresponding eigenvalue matrix follow as

$$V = E\left(E^T E\right)^{-1/2} , \quad \alpha_1 \lambda_1^2 k I_{m-4} . \tag{53}$$

Third step: we know that the number of remaining eigenvectors equals $m - (1 + (m-4)) = 3$. We also know that these eigenvectors satisfy $x \in R(e_m)^{\perp} = R(D)$ and $x \perp z$ for $\bar{A}^T P z = 0$, $z = Dy$. Vectors in the range space $R(P\bar{A})$ are clearly orthogonal to z and also lie in $R(D)$. It therefore follows, since $\dim R(P\bar{A}) = 3$, that the last three eigenvectors span $R(P\bar{A})$. In order to find the corresponding eigenvalues, let $x = P\bar{A}a$ for some $a \in R^3$. Substitution into Eq. (51) then gives

$$\begin{aligned}
&\alpha_1 \lambda_1^2 k \left[P - \alpha_1 k P \bar{A} Q_{\hat{b}}(\phi,p) \bar{A}^T P\right] P\bar{A}a = \lambda P \bar{A} a , \\
&P\bar{A}\left[(\alpha_1 \lambda_1^2 k - \lambda) I_3 - \alpha_1^2 \lambda_1^2 k^2 Q_{\hat{b}}(\phi,p) \bar{A}^T P \bar{A}\right] a = 0 , \\
&P\bar{A} F^{-T} \left[(\alpha_1 \lambda_1^2 k - \lambda) I_3 - \frac{\alpha_1 \lambda_1^2 k}{\epsilon + 1} (I_3 - \Gamma^{-1})\right] F^T a = 0 ,
\end{aligned}$$

since $\alpha_1 k Q_{\hat{b}}(\phi,p) \bar{A}^T P \bar{A} = \frac{1}{\epsilon+1} F^{-T} (I_3 - \Gamma^{-1}) F^T$, according to Theorem 7 of *Part I*. It thus follows that $a = F^{-T} c_i$ or $x = P\bar{A} F^{-T} c_i$, with the eigenvalues $\lambda_i = \alpha_1 \lambda_1^2 k (\epsilon \gamma_i + 1)/(\epsilon + 1)\gamma_i$, $i = 1,2,3$. The matrix of remaining orthonormal eigenvectors, with its corresponding matrix of eigenvalues, therefore reads

$$U = P\bar{A} F^{-T} \left(F^{-1} \bar{A}^T P \bar{A} F^{-T}\right)^{-1/2} , \quad \frac{\alpha_1 \lambda_1^2 k}{\epsilon + 1} \Gamma^{-1} (\epsilon \Gamma + I_3) . \tag{54}$$

Collecting Eqs. (52), (53), and (54) concludes the proof of the theorem.
End of proof. □

Proof of Theorem 2 (*Canonical form of L_1/L_2 search space*)
Although it is possible to give a constructive proof along the lines of the proof of Theorem 1, we will now simply show how the theorem can be verified. It is easily verified that matrix R_{12} is orthogonal. What remains to be verified is therefore

$$\begin{aligned}
&R_{12}^T (I_2 \otimes D) Q_{\hat{a}}^{-1} \left(I_2 \otimes D^T\right) R_{12} \\
&\quad = \operatorname{diag}\left(\Lambda_1^{-1}, \Lambda_2^{-1}, \alpha_1 \lambda_1^2 k I_{m-4}, \alpha_2 \lambda_2^2 k I_{m-4}, 0, 0\right) ,
\end{aligned} \tag{55}$$

where, according to Theorem 1 of *Part II*,

$$Q_{\hat{a}} = \begin{bmatrix} Q_{\hat{a}_1} & Q_{\hat{a}_1 \hat{a}_2} \\ Q_{\hat{a}_2 \hat{a}_1} & Q_{\hat{a}_2} \end{bmatrix} , \tag{56}$$

with

$$\begin{cases} Q_{\hat{a}_1} & = \frac{1}{\lambda_1^2}\left[\frac{1}{\alpha_1 k} D^T D + D^T \bar{A} Q_{\hat{b}}(\phi,p)\bar{A}^T D\right] , \\ Q_{\hat{a}_1\hat{a}_2} & = \frac{1}{\lambda_1\lambda_2}\left[D^T \bar{A} Q_{\hat{b}}(\phi,p)\bar{A}^T D\right] , \\ Q_{\hat{a}_2} & = \frac{1}{\lambda_2^2}\left[\frac{1}{\alpha_2 k} D^T D + D^T \bar{A} Q_{\hat{b}}(\phi,p)\bar{A}^T D\right] . \end{cases}$$

Since

$$R_{12}^T (I_2 \otimes D) = \begin{bmatrix} I_{2(m-1)} \\ 0 \end{bmatrix} \begin{bmatrix} T^T (I_2 \otimes U^T D) \\ (I_2 \otimes V^T D) \end{bmatrix}$$

and

$$\begin{bmatrix} T^T (I_2 \otimes U^T D) \\ (I_2 \otimes V^T D) \end{bmatrix}^{-1} = \begin{bmatrix} T^T (I_2 \otimes U^T D^{+T}) \\ (I_2 \otimes V^T D^{+T}) \end{bmatrix}^T ,$$

with

$$T = \begin{bmatrix} C & -S \\ S & C \end{bmatrix} \text{ and } D^+ = (D^T D)^{-1} D^T ,$$

we may write

$$R_{12}^T (I_2 \otimes D) Q_{\hat{a}}^{-1} \left(I_2 \otimes D^T\right) R_{12} = \begin{bmatrix} I_{2(m-1)} \\ 0 \end{bmatrix} \begin{bmatrix} X & Y \\ Y^T & Z \end{bmatrix}^{-1} \begin{bmatrix} I_{2(m-1)} \\ 0 \end{bmatrix}^T ,$$

where

$$\begin{cases} X = T^T (I_2 \otimes U^T D^{+T}) Q_{\hat{a}} (I_2 \otimes D^+ U) T , \\ Y = T^T (I_2 \otimes U^T D^{+T}) Q_{\hat{a}} (I_2 \otimes D^+ V) , \\ Z = (I_2 \otimes V^T D^{+T}) Q_{\hat{a}} (I_2 \otimes D^+ V) . \end{cases}$$

Since the matrix (U, V, w) is orthogonal according to Theorem 1, with the range spaces $R(U) = R(P\bar{A})$ and $R(V) = R(P\bar{A}, e_m)^\perp$, and since

$$\begin{cases} Q_{\hat{b}}(\phi,p) = \left[F\left(\epsilon I_3 + \Gamma^{-1}\right)^{-1} F^T\right]^{-1} , \\ \bar{A} P \bar{A} & = \epsilon \frac{1}{(\beta_1+\beta_2)k} F\left(I_3 - \Gamma^{-1}\right) F^T , \end{cases}$$

according to Theorem 7 of *Part I*, it follows with Eq. (56) that

$$\begin{cases} X = \begin{bmatrix} C & S \\ -S & C \end{bmatrix} \begin{bmatrix} \Sigma_1 & \Sigma_{12} \\ \Sigma_{12} & \Sigma_2 \end{bmatrix} \begin{bmatrix} C & -S \\ S & C \end{bmatrix} , \\ Y = 0 , \\ Z = \begin{bmatrix} \frac{1}{\alpha_1 \lambda_1^2 k} I_{m-4} & 0 \\ 0 & \frac{1}{\alpha_2 \lambda_2^2 k} I_{m-4} \end{bmatrix} , \end{cases}$$

with

$$\begin{cases} \Sigma_1 & = \frac{1}{\lambda_1^2}\left[\frac{1}{\alpha_1 k} I_3 + \frac{1}{(\alpha_1+\alpha_2)k}(I_3 + \epsilon\Gamma)^{-1}(\Gamma - I_3)\right] , \\ \Sigma_{12} & = \frac{1}{\lambda_1\lambda_2}\left[\frac{1}{(\alpha_1+\alpha_2)k}(I_3 + \epsilon\Gamma)^{-1}(\Gamma - I_3)\right] , \\ \Sigma_2 & = \frac{1}{\lambda_2^2}\left[\frac{1}{\alpha_2 k} I_3 + \frac{1}{(\alpha_1+\alpha_2)k}(I_3 + \epsilon\Gamma)^{-1}(\Gamma - I_3)\right] . \end{cases}$$

Hence, what remains to be shown is that

$$\begin{cases} C^2\Lambda_1 + S^2\Lambda_2 = \Sigma_1 , \\ CS(\Lambda_1 - \Lambda_2) = \Sigma_{12} , \\ S^2\Lambda_1 + C^2\Lambda_2 = \Sigma_2 . \end{cases}$$

But since all matrices in these three matrix equations are diagonal, these equations are easily verified.
End of proof. □

References

de Jonge PJ, Tiberius CCJM (1995) *Integer ambiguity estimation with the LAMBDA method. Proc. IAG Symp 115 'GPS trends in terrestrial, airborne and spaceborne applications'*, XXI General Assembly of IUGG, July 2–14, Boulder, Co, Springer, Berlin Heidelberg, New York, pp 280–284

Teunissen PJG (1994) A new method for fast carrier phase ambiguity estimation. *Proc IEEE PLANS'94*, Las Vegas, NV, April 11–15, pp 562–573

Teunissen PJG (1996a) Part I: The Baseline Precision. Submitted to *J Geod*

Teunissen PJG (1996b) Part II: The Ambiguity Precision and Correlation. Submitted to *J Geod*

Teunissen PJG (1996c) GPS Carrier Phase Ambiguity Fixing Concepts. In: Kleusberg A, Teunissen PJG (Eds), GPS for Geodesy, Springer, Berlin Heidelberg New York, pp 263–335

Tiberius CCJM, de Jonge PJ (1995) Fast positioning using the LAMBDA method. *Proc 4th Int Symp Differential Satellite Navigation Systems DSNS'95*. Bergen, Norway, April 24–28. Paper No. 30, pp 8